



ALMA MATER STUDIORUM  
UNIVERSITÀ DI BOLOGNA

ARCHIVIO ISTITUZIONALE  
DELLA RICERCA

## Alma Mater Studiorum Università di Bologna Archivio istituzionale della ricerca

A Comparison Between Organic Rankine Cycle and Supercritical CO<sub>2</sub> Bottoming Cycles for Energy Recovery From Industrial Gas Turbines Exhaust Gas

This is the final peer-reviewed author's accepted manuscript (postprint) of the following publication:

*Published Version:*

Ancona, M.A., Bianchi, M., Branchini, L., De Pascale, A., Melino, F., Peretto, A., et al. (2021). A Comparison Between Organic Rankine Cycle and Supercritical CO<sub>2</sub> Bottoming Cycles for Energy Recovery From Industrial Gas Turbines Exhaust Gas. JOURNAL OF ENGINEERING FOR GAS TURBINES AND POWER, 143(12), 1-11 [10.1115/1.4051950].

*Availability:*

This version is available at: <https://hdl.handle.net/11585/869238> since: 2022-09-22

*Published:*

DOI: <http://doi.org/10.1115/1.4051950>

*Terms of use:*

Some rights reserved. The terms and conditions for the reuse of this version of the manuscript are specified in the publishing policy. For all terms of use and more information see the publisher's website.

This item was downloaded from IRIS Università di Bologna (<https://cris.unibo.it/>).  
When citing, please refer to the published version.

(Article begins on next page)



ASME Accepted Manuscript Repository

Institutional Repository Cover Sheet

---

*First*

*Last*

ASME Paper Title: A comparison between ORC and supercritical CO<sub>2</sub> bottoming cycles for energy recovery industrial gas turbines exhaust gas

Authors: Ancona M. A.; Bianchi M.; Branchini L.; De Pascale A.; Melino F.; Peretto A.; Torricelli N.

ASME Journal Title: ASME Turbo Expo 2021: Turbomachinery Technical Conference and Exposition

Volume/Issue Volume 7

Date of Publication (VOR\* Online): September 16, 2021

ASME Digital Collection URL: <https://asmedigitalcollection.asme.org/GT/proceedings/GT2021/85000/V007T16A004>

DOI: <https://dx.doi.org/10.1115/GT2021-59180>

\*VOR (version of record)

---

# A COMPARISON BETWEEN ORC AND SUPERCRITICAL CO<sub>2</sub> BOTTOMING CYCLES FOR ENERGY RECOVERY FROM INDUSTRIAL GAS TURBINES EXHAUST GAS

M. A. Ancona, M. Bianchi, L. Branchini, A. De Pascale, F. Melino, A. Peretto, N. Torricelli\*

Alma Mater Studiorum University of Bologna – Department of Industrial Engineering (DIN),  
Viale del Risorgimento 2, 40136 Bologna, Italy

## ABSTRACT

Gas turbines are often employed in the industrial field, especially for remote generation, typically required by oil and gas production and transport facilities. The huge amount of discharged heat could be profitably recovered in bottoming cycles, producing electric power to help satisfying the onerous on-site energetic demand. The present work aims at systematically evaluating thermodynamic performance of ORC and supercritical CO<sub>2</sub> energy systems as bottomer cycles of different small/medium size industrial gas turbine models, with different power rating. The Thermoflex software, providing the GT PRO gas turbine library, has been used to model the machines performance. ORC and CO<sub>2</sub> systems specifics have been chosen in line with industrial products, experience and technological limits.

In the case of pure electric production, the results highlight that supercritical CO<sub>2</sub> configuration shows the highest plant net electric efficiency, when combined with small size turbines; when considering instead larger size turbines, it is ORC configuration to show higher performance. The average increment in the overall net electric efficiency is promising for both the configurations (9 and 11 percentage points, respectively if considering supercritical CO<sub>2</sub> or ORC as bottoming solution). Concerning the cogenerative performance, the CO<sub>2</sub> system exhibits at the same time higher electric efficiency and thermal efficiency, if compared to ORC system, being equal the installed topper gas turbine model. The ORC scarce performance is due to the high condensing pressure, imposed by the temperature required by the thermal user. CO<sub>2</sub> configuration presents instead very good cogenerative performance with thermal efficiency comprehended between 35 % and 45 % and the PES value range between 10 % and 20 %. Finally, analyzing the relationship between capital cost and components size, it is estimated that the CO<sub>2</sub> configuration could introduce an economical saving with respect to the ORC base configuration.

Keywords: organic Rankine cycle, CO<sub>2</sub> supercritical, gas turbine, oil and gas application, waste heat recovery.

## NOMENCLATURE

### Abbreviation

COG	Cogenerative
CF	Correction Factor

GT	Gas Turbine
HX	Heat Exchanger
LHV	Lower Heating Value
ORC	Organic Rankine Cycle
s-CO <sub>2</sub>	supercritical CO <sub>2</sub> cycle
TIT	Turbine inlet temperature

### Symbols

$A$	Surface area (m <sup>2</sup> )
$C$	Investment cost (€)
$F$	Power introduced with fuel (W)
$h$	Enthalpy (J/kg)
$\dot{m}$	Mass flow rate (kg/s)
$P$	Electrical power (W)
$p$	Pressure (bar)
$Q$	Thermal power (W)
$SP$	Expander size parameter (m)
$s$	Entropy (J/kg/K)
$T$	Temperature (°C)
$U$	Global heat transfer coefficient (W/m <sup>2</sup> /K)

### Subscripts

bott	Bottomer cycle
cool	Cooling medium
ex	Exhaust gas
is	Isentropic
in	Inlet
max	Maximum
misc	Miscellaneous
out	Outlet
ref	Reference

### Greek letters

$\alpha$	Convective heat transfer coefficient (W/m <sup>2</sup> /K)
$\beta$	Pressure ratio (-)
$\eta$	Electrical efficiency (%)
$\tau$	Thermal efficiency (%)

## INTRODUCTION

Given its flexibility, gas turbine (GT) technology in simple cycle arrangement is widely diffused and employed in relevant industrial applications. In this case the energy system is stationary and the shaft power is directly used on-site, in mechanical drive applications, or converted into electrical power, to satisfy electric users. Unfortunately LHV electric efficiency is limited to values up to 40-45 % achieved by the

most performing large size aeroderivative machines, but small/mid-power industrial machines typically show efficiency values in the range of 20-35 %, resulting in a huge amount of thermal energy rejected with exhaust gases [1]. This wasted energy could be considered as a secondary resource to be exploited to generate additional electric energy or/and heat in cogeneration units. The aim is to increase the primary energy utilization and consequently to limit energy generation costs and emissions.

Waste heat recovery potential from GT exhaust gas is believed to be significant in many energy intensive industries [2]. In particular, one of the most promising industrial context is the oil-and-gas sector, where multi-unit arrangements GTs are currently utilized in natural gas compression stations and off-shore applications. In this case, the temperature of the GT exhaust can be on average equal to 450 – 500 °C, while the flow rates range between 5 to 100 kg/s. Nevertheless, single unit GTs employed in natural gas compressor stations and other industrial applications are commonly limited in size and regularly operate under part-load conditions to follow the fluctuating energy demand. Thus, exhaust temperature and mass flow values are not always compatible to traditional steam bottoming cycle. Rather than deploying a steam plant, more appropriate alternatives might consist in simpler and more flexible bottoming systems, such as the well-established organic Rankine cycle (ORC) and the innovative supercritical CO<sub>2</sub> based Brayton cycle (s-CO<sub>2</sub>). Both these thermodynamic solutions rely on operating fluids with critical temperatures lower than water and other common positive characteristics are: i) the dry expansion; ii) the simple generation of the vapour at the turbine inlet (only a heat exchanger is needed); iii) the possibility to operate with air-cooled condenser [3].

ORC systems are already available on the market and successfully employed for industrial waste heat recovery. Several companies have been actively pursuing natural gas compressor stations heat recovery over the past several years. For instance, Ormat has currently a dozen compressor recovery systems and processing plants in operation in the North America, with as many additional ones in construction [4], for more than 50 MWe installed. Turboden also has operating plants since 2011 and others under construction for a total of about 10 MW in oil and gas [5] and of about 26 MW in combined cycles with gas turbines and engines, and continues investigating innovative solutions [6]. Conversely, supercritical CO<sub>2</sub> cycle is also known for a long time, but it has not yet been developed, due to technological limits, nevertheless recently advances in technology promise to make it practical and re-ignite the interest in CO<sub>2</sub> power cycle.

Several studies investigate s-CO<sub>2</sub> potential for high-temperature heat recovery, mostly concerning solar and nuclear applications, and still poorly fossil fuels applications [7]. Some examples are: i) Turchi et Al. [8], whom comprehensively analyzed thermodynamic performance of concentrating solar supercritical CO<sub>2</sub> power cycles; ii) Sybilik et Al. [9], whom focused on design optimization for nuclear and fusion energy sector; iii) Park et Al. [10], whom explore thermodynamic and

economic aspects of coal-fired combined power plant with CO<sub>2</sub> based Brayton cycle.

Instead, the research is still scarce regarding the medium-to-low temperature CO<sub>2</sub> power cycles applications, although s-CO<sub>2</sub> technology may be considered competitive with ORC solution in this operating range. Indeed it has the valuable advantage of using non-toxic, nonflammable, environmental friendly and widely available working fluid [11].

It must be cited the study of Astolfi et Al. [12], comparing CO<sub>2</sub> power cycles and ORC for waste heat recovery applications, providing performance maps, as function of different heat sources maximum temperature (200-600 °C) and cooling grades. The Authors demonstrated that the most convenient choice sensibly depend on the actual boundary conditions. However, except for this work, literature lacks of studies regarding industrial applications of CO<sub>2</sub> based waste heat recovery and specific comparison with ORC, in particular in more realistic operating conditions. For example, the bottoming solutions of small/medium gas turbines for electric and thermal industrial applications could be an interesting application to be explored.

In order to fulfill this knowledge gap, this paper proposes to investigate and compare thermodynamic performance of ORC and s-CO<sub>2</sub> systems as bottoming of selected GT models, typically employed in oil and gas infrastructures. For this purpose, the Thermoflex commercial software [13], providing the GT PRO gas turbine library, has been used for the simulations. The ORC and s-CO<sub>2</sub> systems specifics have been chosen in line with industrial products and state-of-the-art research experience, as described below. A systematic analysis has been performed, considering pure electric and combined heat and power plant configurations, discussing energetic results in terms of electric and thermal power production, efficiency, primary energy savings, components dimensions and costs.

# 1 HEAT RECOVERY CONFIGURATIONS

In this study, the organic Rankine cycle and the supercritical CO<sub>2</sub> cycle are analyzed as bottomer of gas turbines and compared in different heat recovery configurations. More in specific, the considered s-CO<sub>2</sub> bottoming cycle is a thermodynamic variant of the Brayton closed cycle arrangement. In particular, a simple recuperated cycle is considered, a basic setup avoiding other more complicated arrangements, introduced in previous studies on s-CO<sub>2</sub> cycles, indicated as more performing especially with high temperature of the hot source [14]. The ORC subcritical recuperated architecture is chosen as

comparative bottoming system, according to the current state of the art of waste heat recovery applications [3]. Direct heat recovery solution, without intermediate heat transfer fluid between the GT exhaust and the organic fluid, is considered.

FIGURE 1 illustrates the heat recovery configurations in exam, all comprehending a gas turbine topper energy system and a bottoming power plant. Nevertheless, the ORC and the s-CO<sub>2</sub> bottoming systems operate with very different boundary conditions (as better described in the “MODELLING ASSUMPTION” paragraph), the two systems are composed by some common components, as listed below:

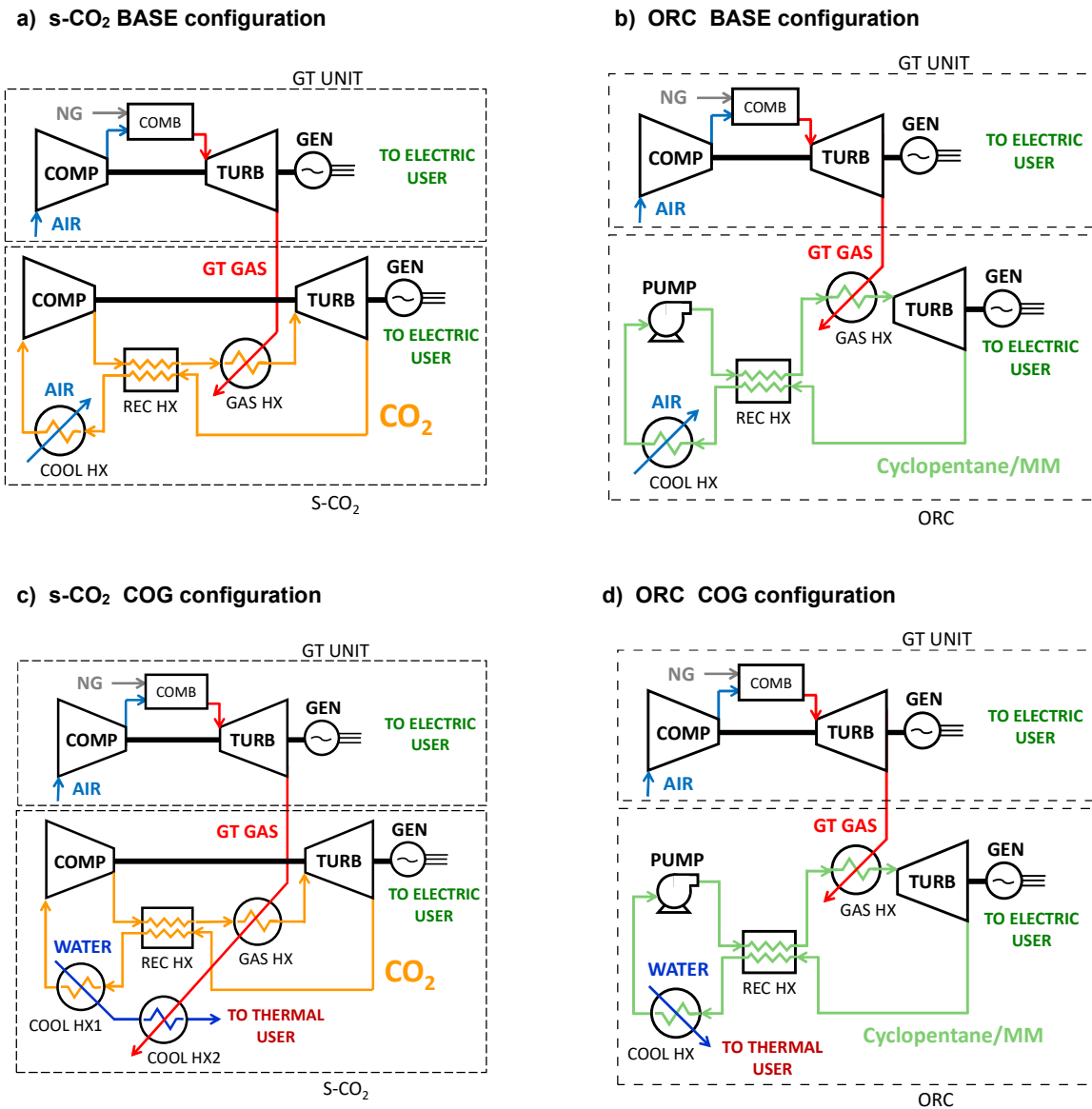


**FIGURE 1: ANALYZED CONFIGURATIONS LAYOUTS:**  
a) s-CO<sub>2</sub> base, b) ORC base, c) s-CO<sub>2</sub> cogenerative, d) ORC cogenerative.

- a heat exchanger (“GAS HX”), in which the high temperature GT exhaust gas are conveyed to provide heat to the working fluid circulating in the bottoming cycle.
- a turbine, in which the working fluid expands to produce mechanical work, converted into electricity by a generator.
- a recuperator (“REC HX”), to recover part of the working fluid exhaust heat to pre-heat the fluid before the GAS HX inlet.
- a cooling heat exchanger (“COOL HX”), which has the task of subtracting heat from the exhaust working fluid.
- an operating machine, to increase the working fluid pressure. It can be a pump or a compressor, respectively if considering the ORC configuration or the s-CO<sub>2</sub> cycle.

These two kinds of heat recovery configurations are in their turn simulated in two different scenarios, assuming different boundary conditions:

- a **“BASE” scenario**, considering the pure electric energy production. In this configuration, the bottoming cycle provides only electric energy to the user. The chosen cooling medium is ambient air, as more suitable for water-scarce environments, such as remote installations.
- a **cogenerative scenario (“COG”)** involving both the electric and the thermal energy production. This configuration requires an electric consumer as well as a thermal user. The layout difference between COG and BASE option is in the use of water in a closed-loop configuration, despite of ambient air, as cooling medium in COOL HX. In this case, the presence of water is justified by its use into a hot water circuit providing heat to the thermal user. It can be noticed that COG-CO<sub>2</sub> configuration involves two COOL HXs, the second one (COOL HX2) placed downstream GAS HX. The aim of COOL HX2 is to further cool down GT exhaust gas and provide additional thermal power to the hot water circuit at the same time. More detail on this assumption are given in the “MODELLING ASSUMPTION” paragraph.

## 2 MODELLING ASSUMPTIONS

The power plant, comprehending the gas turbine and the bottomer cycle, has been modelled by means of the commercial software Thermoflex [13]. The software allows for the thermodynamic modelling of complex power plants, starting from built-in library single components assembly, using a lumped parameters approach.

In particular, the software’s GT PRO gas turbine library, has been used to simulate commercial gas turbines. The involved organic fluids and CO<sub>2</sub> properties are evaluated according to Refprop thermodynamic database [17].

A detailed description of the modeling assumptions for each system is reported in the following paragraph, presenting: i) gas turbine specifics and other boundary conditions, ii) supercritical CO<sub>2</sub> cycle specifics, iii) ORC system specifics. The s-CO<sub>2</sub> and ORC specifics have been chosen in line with industrial products,

experience and technological limits. Instead, the bottoming cycle maximum operating pressure value, which is a key cycle design parameter, comes as results of a parametric analysis (as detailed in paragraph 2.4).

### 2.1 Gas turbines selection and boundary conditions

Wide-ranging power ratings GTs can be found in industrial applications, where small and mid-size machines are often used in more flexible multiple arrangements. Indeed, smaller power rating units (MW size range) are often installed on-board of small production facilities, e.g. in off-shore plants. Larger power rating units (ranging up to tens of MW), both heavy-duty and aeroderivative machines, can be used on larger facilities requiring higher power needs [15]. Thus, four different GT power sizes have been investigated in this study, namely 1MW, 5MW, 15MW and 30MW, in order to cover a wide spectrum of small/mid-size industrial GT applications, in line with previous studies referring to the oil and gas sector [14, 15].

The selected GT units design data are summarized in TABLE 1. Limited GT electric efficiency value can be observed (24 %) for the smallest power rated unit (Kawasaki GPB15), around 30-33% for larger power rated units and up to 36% for Siemens GT 700 machine. In particular, the following two points, influencing the available thermal power in the exhaust, can be noticed: i) exhaust gas mass flow rate raises with the gas turbine size and it ranges between 8 and 89 kg/s for the selected GTs; ii) exhaust gas temperature is limited in a quite narrow range centered around 500-550°C, varying between 474 °C and 574 °C for the selected machines.

TABLE 1: GAS TURBINES NOMINAL DATA.

	$P_{GT}$ (MW)	$TIT_{GT}$ (°C)	$\beta_{GT}$ (-)	$\eta_{GT}$ (%)	$\dot{m}_{ex}$ (kg/s)	$T_{ex}$ (°C)
<b>Kawasaki GPB15 GT1</b>	1.5	991	9.4	24.2	8	520
<b>GE5 GT2</b>	5.5	1232	14.8	30.6	19	574
<b>Solar Titan 130 GT3</b>	15	1093	15.7	33.3	49	474
<b>Siemens GT 700 GT4</b>	30	1260	17.6	36	89	518

Additional common boundary conditions for the bottoming cycles are indicated in TABLE 2 and concern:

- hot water temperature requested by the thermal user equal to 90 °C, in cogenerative configuration.
- the temperature of the GT exhaust gases at the GAS HX outlet (exhaust stack). Its value is assumed equal to 125 °C, to maximize the heat transferred to the bottomer section, but still avoiding the cold-end corrosion issues in the exhaust stack. In the COG s-CO<sub>2</sub> configuration, an additional COOL HX2 downstream GAS HX, allows to further cool GT exhaust gas and provide additional thermal power to the hot water circuit at the same time. In this case, two gas heat

exchangers are considered instead of one, in order to get the exhaust gas stack temperature closer to 125 °C (see heat exchangers GAS HX and COOL HX2, in FIGURE 1c). Indeed, it has been observed that a single heat exchanger would not allow to discharge the gas below 250 °C.

**TABLE 2: GENERAL BOUNDARY CONDITIONS.**

General specifics	
Inlet air properties	ISO conditions
Minimum GT stack temperature	125 °C
Miscellaneous efficiency	98 %
Hot water temperature to thermal user (COG configuration)	90 °C
Hot water temperature return from thermal user (COG configuration)	25 °C

## 2.2 Supercritical CO<sub>2</sub> cycle

The s-CO<sub>2</sub> system specifics are selected on the basis of guidelines followed by Crespi et Al. [14], according to s-CO<sub>2</sub> cycles survey, performed by the Authors. Main specifics are listed in TABLE 3 and commented here:

- the compressor inlet temperature and pressure are imposed respectively equal to 35 °C and 75 bar. This choice grants to maintain supercritical conditions all along the cycle, given CO<sub>2</sub> supercritical temperature equal to 31 °C and supercritical pressure equal to 74 bar (see thermodynamic properties illustrated in FIGURE 2).
- the turbine inlet state is determined by the gas exhaust heat exchanger performance and by the cycle maximum pressure. The cycle maximum pressure value comes as result of a parametric analysis which aims at optimizing the plant efficiency. Its value is limited to 300 bar as a consequence of technological limits.
- the turbine and compressor polytropic efficiencies are imposed respectively equal to 88 % and 90 % for CO<sub>2</sub> power plant size lower or higher than 2 MW, in order to account for the machine size-effect over the performance.

**TABLE 3: CO<sub>2</sub> CYCLE SPECIFICS.**

Fluid	Carbon Dioxide
Compressor inlet pressure	75 bar
Compressor inlet temperature	35 °C
Turbine inlet pressure upper limit	300 bar
Turbine and compressor polytropic efficiency ( $P_{bott} < 2 \text{ MW} / P_{bott} > 2 \text{ MW}$ )	88/90 %
Recuperator thermal effectiveness	80 %
Pressure drop across heat exchangers	2 %
Heat exchangers normalized heat loss	1 %
Heat exchangers minimum pinch point	10 °C

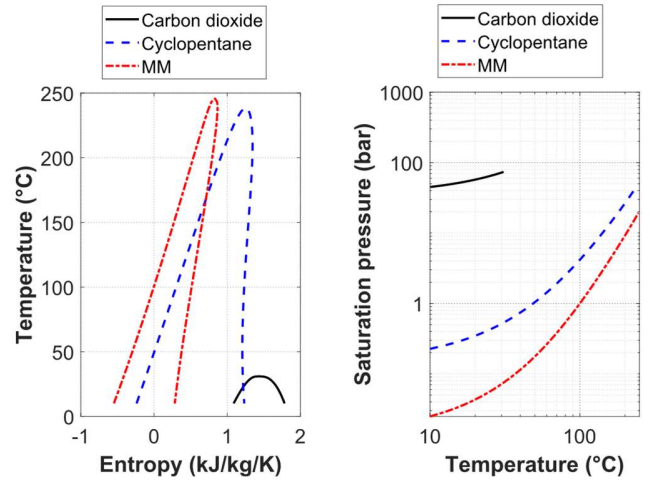


**FIGURE 2: CO<sub>2</sub> AND CYCLOPENTANE PROPERTIES AT SATURATION OBTAINED USING REFPROP LIBRARY [17].**

## 2.3 ORC system

The ORC thermodynamic design data are selected as consistent with existing large-scale industrial well-established products [16] (see TABLE 4). In particular:

- the cyclopentane and the MM are selected as working fluids, respectively for the largest sizes (bottomer cycle power,  $P_{bott} > 2 \text{ MW}$ ) and the smallest size ( $P_{bott} < 2 \text{ MW}$ ). Indeed, these fluids are both commonly used in industrial medium waste heat recovery application, thanks to characteristics such as: i) a critical temperature around 240 °C (see FIGURE 2), compatible with the GT exhaust gas temperature; ii) high molecular weight, fundamental to maintain small size ORC power plant in terms of compactness and economics (i.e. lower investment costs). In particular, MM is preferred for small size applications due to its higher molecular weight (162 kg/kmol against 70 kg/kmol of the cyclopentane), which allow to design the expander machine with a lower number of stages (even single stage turbine) thanks to lower speed of sound. On the other hand, fluids with high molecular weight show small enthalpy drops during expansion.
- the expander inlet state is set to superheated vapour at a temperature determined by the gas exhaust heat exchanger performance and by the cycle maximum pressure. Temperature is conservatively limited to 280 °C, in order to not overcome thermal stability limit corresponding to 300 °C. The cycle maximum pressure (corresponding to the evaporating pressure) value results from the plant efficiency optimization. The maximum pressure value is limited to the 90 % of the critical pressure value, equal to 45.1 bar for the cyclopentane and 19.4 bar for the MM;

- the ORC condenser pressure is influenced by the cooling medium temperature. Therefore, the condensing pressure is considered equal to the fluid saturation pressure value (see FIGURE 2) at: i) 35 °C in the base configuration; ii) 95 °C in the cogenerative configuration. As a consequence, the cogenerative configuration leads to an increase in the condensing pressure value. A lower limit equal to 0.3 bar is imposed for the base configuration using MM, as typically considered limit to contain costs of low-pressure components.

**TABLE 4: ORC SPECIFICS.**

Fluid	MM ( $P_{bott} < 2$ MW)	Cyclopentane ( $P_{bott} > 2$ MW)
Turbine inlet temperature upper limit	280 °C	
Turbine inlet pressure upper limit	17 bar	40 bar
Turbine isentropic efficiency	80 %	85 %
Pump isentropic efficiency	60 %	
Condensing pressure (base/COG solution)	0.3/0.9 bar	0.6/3.7 bar
Condensate subcooling	5 °C	
Heat exchangers minimum pinch point	5 °C	
Pressure drop across heat exchangers	1 %	
Recuperator thermal effectiveness	80 %	

## 2.4 Bottoming cycle maximum pressure

The cycle maximum pressure is a key decision parameter strongly influencing the bottomer performance. Therefore, as first step, a thermodynamic parametric analysis involving the electric power production optimization is conducted to establish the optimal bottoming cycle maximum pressure value.

FIGURE 3 shows the results of the parametric analysis, where the normalized value of the net power output,  $P_{net}$ , normalized with respect to its maximum value, is plotted against the normalized value of the cycle maximum pressure,  $p_{max,bott}$ , normalized with respect to its limiting value. As a result, the cycle maximum pressure values that maximize the power output are found to be equal to their upper limits for both s-CO<sub>2</sub> and ORC systems, which are respectively 300 bar, 40 bar for cyclopentane ORC and 17 bar for MM ORC. Thus, the latter values are imposed as boundary condition for the simulations.

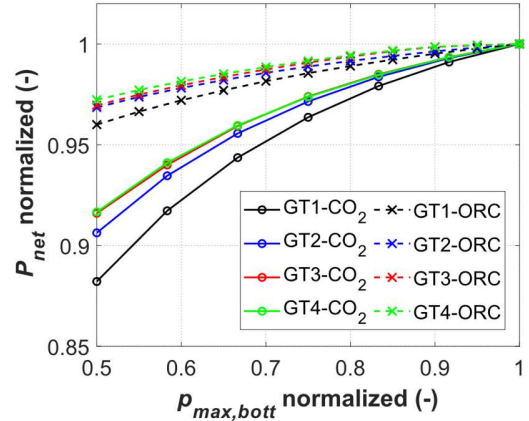


**FIGURE 3: BOTTOMING CYCLES MAXIMUM PRESSURE OPTIMIZATION: NORMALIZED NET OUTPUT POWER VS NORMALIZED MAX PRESSURE.**

## 3 PERFORMANCE AND SIZE INDEXES

In order to carry out a systematic analysis on the proposed configurations, several performance indexes are evaluated to measure and compare the energy production and components size. The most relevant performance indexes used in the analysis are specified below:

- Net electric power ( $P_{net}$ )** is given by the sum of the net electric power generated by the gas turbine,  $P_{GT}$ , and the net electric power generated by bottomer cycle,  $P_{bott}$ , minus the plant miscellaneous absorbed power,  $P_{misc}$  (due to the miscellaneous efficiency, see TABLE 2):

$$P_{net} = P_{GT} + P_{bott} - P_{misc} \quad (1)$$

- Net electric efficiency ( $\eta$ )** is given by the ratio between the net electric power and the GT fuel input power with reference to LHV,  $F$ :

$$\eta = \frac{P_{net}}{F} \quad (2)$$

- Expander/operating machine available isentropic power ( $P_{is}$ )** is given by the difference between the machine inlet enthalpy,  $h_{in}$ , and the value the enthalpy would have at the machine outlet if the process were isentropic,  $h_{out,is}$ , multiplied to the fluid mass flow rate,  $\dot{m}$ . The isentropic outlet condition is evaluated at the machine outlet pressure,  $p_{out}$ , and machine inlet entropy,  $s_{in}$ .

$$P_{is} = \dot{m} \cdot (h_{in} - h_{out,is}(s_{in}, p_{out})) \quad (3)$$



Isentropic power is a useful thermodynamic index to evaluate theoretical power available for the expansion process or absorbed by the operating machine.

- **Bottoming cycle thermal power input ( $Q_{gas,HX}$ )** is calculated as the product of GT exhaust gas mass flow rate, and the enthalpy difference through the gas heat exchanger (GAS HX).
- **Bottoming cycle discharged thermal power ( $Q_{cool,HX}$ )** is calculated as the product of the cooling mass flow rate, and the enthalpy difference through the cooling heat exchangers (COOL HX).
- **Recovered thermal power for cogenerative purpose ( $Q_{cog}$ )** is calculated as the product of cooling medium mass flow rate and the enthalpy difference through the cogenerative heat exchangers. It corresponds to  $Q_{cool,HX}$  value in the ORC cogenerative case, whilst, for CO<sub>2</sub> configuration, it corresponds to  $Q_{cool,HX}$  plus a thermal power contribution recovered from exhaust gas in COOL HX 2, as illustrated in FIGURE 1c.
- **Thermal efficiency ( $\tau$ )** is given by the ratio between the recovered thermal power and the GT fuel inlet power,  $F$ :

$$\tau = \frac{Q_{cog}}{F} \quad (4)$$

- **Primary energy saving (PES)** is a quite common performance indicator for cogenerative energy systems and accounts for both the electric and the thermal production. In particular, the PES represents the energy savings of the considered combined heat and power plant with respect to a reference scenario of separate electric and thermal production. The reference electricity is supposed to be generated with a conventional pure electric system having an electric efficiency  $\eta_{ref}$  and the reference thermal production is generated with a standalone heat generator with thermal efficiency equal to  $\tau_{ref}$ . The reference values selected for electric efficiency and thermal efficiency are 52.5 % and 90 %, respectively [18].

$$PES = 1 - \frac{1}{\frac{\eta}{\eta_{ref}} + \frac{\tau}{\tau_{ref}}} \quad (5)$$

Besides performance considerations, it may be also important to take into account some design aspects related to the investment cost and the space requirements. For this purpose, a preliminary analysis concerning the size of key components (heat exchangers and expander) is also presented. The following parameters are computed in a second step, as function of the performance results obtained by means the Thermoflex software:

- **The heat exchanger size parameter ( $A$ )** is defined as the heat exchanger surface area, as function of the global heat transfer coefficient,  $U$ , the exchanged thermal power,  $Q$ , and the heat exchanger mean logarithmic temperature difference,  $\Delta T_{ml}$ , for a given heat exchanger:

$$A = \frac{Q}{U \cdot \Delta T_{ml}} \quad (6)$$

The total heat exchangers size parameter,  $A_{tot}$ , then, is also evaluated as the sum of surface areas of the single heat exchangers, namely: “GAS HX”, “REC HX and “COOL HX”, respectively indicating the GT gas heat recovery heat exchanger, the recuperator and the heat exchangers employed for cooling/cogenerative purpose.

The global heat transfer coefficient is computed as function of the convective coefficients of the two fluids involved into the heat exchange process, neglecting the conductive contribution at the wall:

$$U = \left( \frac{1}{\alpha_1} + \frac{1}{\alpha_2} \right)^{-1} \quad (7)$$

Assuming fully developed turbulent flow in forced convective regime, Dittus-Boelter correlations is used to estimate the convective heat transfer coefficients,  $\alpha_1$  and  $\alpha_2$ :

$$Nu = 0.023 \cdot Re^{0.8} \cdot Pr^{0.4} \quad (8)$$

where  $Nu$ ,  $Re$  and  $Pr$  represent respectively the Nusselt, the Reynolds and the Prandtl adimensional numbers. Hydraulic diameter value, necessary to calculate  $Re$ , is assumed equal to 2 cm, in line with Standards of the Tubular Heat Exchanger Manufacturers Association [19].

- **The expander size parameter ( $SP$ )** is proposed to evaluate expander size as function of the fluid operating condition inside the machine. This nondimensional index is defined as the ratio between the fluid volume flow rate evaluated at the expander outlet pressure, and the isentropic enthalpy drop trough the expander,  $\Delta h_{is}$  [20]. The volume flow rate is given by the ratio between the fluid mass flow rate,  $\dot{m}$ , and its density,  $\rho_{out,is}$ .

$$SP = \frac{(\dot{m} \cdot \rho_{out,is})^{0.5}}{\Delta h_{is}^{0.25}} \quad (9)$$

A simplified estimation of the investment cost has been also performed, considering the most expensive components in a heat recovery system, i.e. the heat exchangers and the expander.

- a **capital cost parameter,  $C_{tot}$** , is defined as the sum of the heat exchangers ( $C_{gas}$ ,  $C_{rec}$ ,  $C_{cool}$ ) and the turbine investment cost,  $C_{turb}$ . The investment cost for each

component,  $C_i$ , can be evaluated by using the standard formula [19]:

$$C_i = C_0 \left( \frac{SP_i}{SP_0} \right)^n \cdot CF(p_{max,bott}) \quad (10)$$

according to which, a reference cost value,  $C_0$ , is scaled by the ratio between the actual size parameter,  $SP_i$ , and the reference size parameter,  $SP_0$ . An exponent,  $n$ , is applied to the scaling factor and the effect of the maximum cycle pressure,  $p_{max,bott}$ , can be accounted through a correction factor  $CF$ . In this analysis, the coefficients and the cost reference values are the ones provided by [21], chosen in line with data for organic fluid-based plants.

It must be highlighted that the proposed design analysis does not aim at defining the exact dimensions and capital costs of the heat exchangers and expander components. The aim is instead to provide order of magnitude of these values, to make comparisons among the different heat recovery configurations in exam.

## 4 RESULTS AND DISCUSSION

This paragraph presents and discusses the results of a comparative analysis, considering plant performance, bottoming cycle components size and capital costs. Compared configurations (as detailed in the previous paragraphs) include:

- different gas turbine models (see TABLE 1);
- different bottoming solutions: supercritical CO<sub>2</sub> cycle and organic Rankine cycle;
- different heat recovery configurations: involving electric power production only and combined heat power plant (see schemes in FIGURE 1).

### 4.1 Performance

#### 4.1.1 Base configuration

First of all, results are presented for the pure electric (BASE) case. The bottomer inlet/discharged HX thermal power values and the expansion/compression isentropic power values results are reported respectively in FIGURE 4 and FIGURE 5; these are key components results influencing the net electric efficiency performance of the ORC and s-CO<sub>2</sub> configurations, as reported in FIGURE 6.

In particular, FIGURE 4 shows that the amount of thermal power that can be recovered from the bottoming cycles range between 2 and 40 MW (GAS HX), for the analyzed GTs topper systems. The amount of exchanged heat increases with the topper gas turbine size, mainly due to the increasing of the gas turbine exhaust gas flow with the size. It must be noticed that higher involved thermal power values are observed for the ORC solution, mainly because of the higher convective heat transfer coefficient of cyclopentane and MM into the evaporator and the condenser, also due to the fluid phase change. This aspect, in

particular, will affect the size of the heat exchangers and associated costs.

FIGURE 5 shows the isentropic power values for both the expander and the operating machine, for the different bottoming solutions, combined with the different examined GTs. Results show that despite the ORC exhibit higher recovered thermal power values, the CO<sub>2</sub> solution presents higher isentropic power values available at the expander, due to high pressure ratios. However, the net power production depends not only by the expander output power but also by the operating machine power absorption, and s-CO<sub>2</sub> configurations exhibit also higher power required by the operating machine. It can be observed that the operating machine isentropic power is equal to the 30 % and 3 %, of the expander isentropic power, for the s-CO<sub>2</sub> and ORC configuration respectively.

In terms of the net isentropic available power (and of the resulting bottoming cycle net specific work per unit of GT exhaust) two scenarios can be distinguished: i) when considering small-size GTs (GT1 and GT2), the available net isentropic power is higher if employing the s-CO<sub>2</sub> system; ii) instead, when considering larger size GTs (GT3 and GT4), the available net isentropic power is higher with the ORC system. This dissimilar result depends on the different ORC operating parameters, for the different TG sizes. In particular, the choice of employing MM as ORC working fluid for small-size GTs affects the operating pressure and as a consequence the enthalpy drop at the expander.

These results on output power obviously affects also the net electric efficiency of the plant, as in FIGURE 6. The s-CO<sub>2</sub> cycle is the configuration showing the highest plant net electric efficiency, when combined with small size turbines (GT1 and GT2); when considering instead larger size turbines (GT3 and GT4), the ORC configuration shows the better performance. It must be noticed that both the analyzed cycle configurations lead to a remarkable increment in the overall net electric efficiency of the power plant, if compared to the GT simple cycle (green line in FIGURE 6). The achieved average increment in efficiency ranges from 9 and 11 percentage points, respectively if considering s-CO<sub>2</sub> or ORC as bottoming solution. In terms of absolute values, it is observed that net electric efficiency value of the integrated systems increases with the topper gas turbine size. This is mainly due to the increase of the simple cycle GT efficiency with size. In particular, the net electric efficiency value of the combined GT/ORC cycle in pure electric configuration reaches its maximum at 48 %, by combining the ORC optimal design with Siemens GT 700 (GT4) model. The GT/s-CO<sub>2</sub> integrated system in pure electric case achieves efficiency values almost close to 45% with GT4.

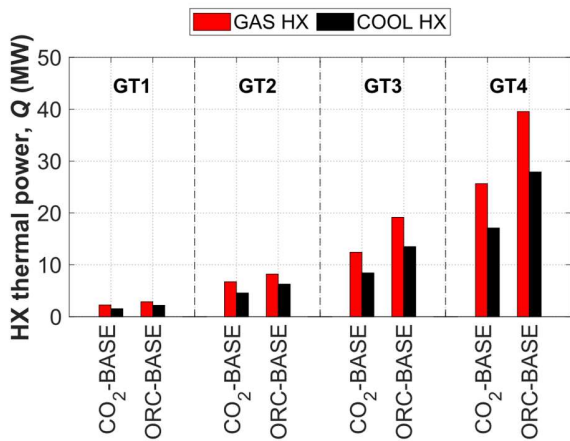


**FIGURE 4:** INLET/OUTLET THERMAL POWER TO THE BOTTOMING CYCLE (BASE CASE).

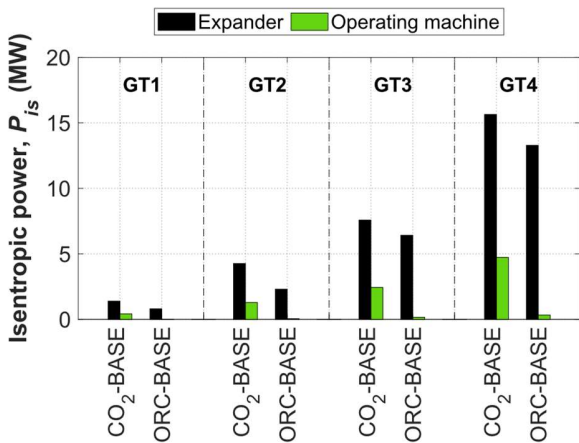


**FIGURE 5:** EXPANDER AND OPERATING MACHINE ISENTROPIC POWER (BASE CASE).

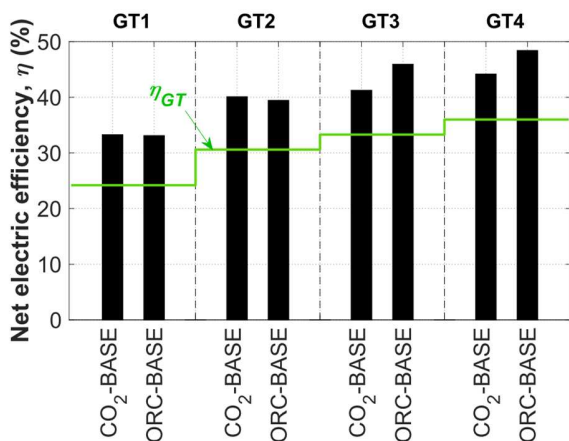


**FIGURE 6:** NET ELECTRIC EFFICIENCY OF THE SYSTEM (BASE CASE).

#### 4.1.2 Cogenerative configuration

The calculated performance results of the COG case are shown in FIGURE 7a; the electrical efficiency and thermal efficiency points of the analyzed configurations are shown, and constant PES lines are also traced in green in the same graph. The electrical efficiency increases with the GT size; the thermal efficiency generally decreases by increasing the GT size, due to the consequent decreasing discharged heat. The GT2 case with s-CO<sub>2</sub> configuration however shows quite a high thermal efficiency value, due to the high GT2 exhaust temperature (574 °C) compared to all the other considered machines, and due to the second HX for heat recovery. The calculated values of thermal efficiency range between 35 % and 45 %. The corresponding PES values are increasing with the GT size and largely positive in many cases (up to 20% for GT4 with s-CO<sub>2</sub> cycle). The achievable primary energy savings are attractive in most of the cases. Only in case of GT1 and with ORC as bottomer the COG configuration becomes less attractive, showing PES close to 0.

It can be observed that the s-CO<sub>2</sub> COG systems exhibit both higher electric efficiency and higher thermal efficiency, if compared to ORC systems, for all the examined topper GT models. This leads to larger PES values in case of the combined GT/s-CO<sub>2</sub> cycles that in case of the GT/ORC systems.

Thermodynamic diagrams of the s-CO<sub>2</sub> and ORC systems as bottomer of GT4 are shown in FIGURE 8 and FIGURE 9, to help explaining the main factors influencing the performance of the two systems in COG configuration.

The CO<sub>2</sub> COG higher thermal efficiency is a consequence of the additional contribution due the second heat exchanger recovering heat from the exhaust GT gas (COOL HX2). The corresponding heat exchange diagram shown in FIGURE 8 reveals indeed that up to 11 MW additional thermal power can be recovered, combining the s-CO<sub>2</sub> cycle with GT4.

The s-CO<sub>2</sub> solution also provides better performance in terms of electric power production; indeed, the ORC electric performance in COG case are negatively affected by the increase of the condensing pressure (see FIGURE 9), leading to a not negligible reduction of the enthalpy drop at the ORC expander. The electric efficiency value decrease of about 4 percentage points if compared with ORC pure electric case. On the contrary, the s-CO<sub>2</sub> base and COG configurations do not considerably differ, because the cooling medium temperature has no effect on the cycle pressures (see CO<sub>2</sub> thermodynamic diagram in FIGURE 8).

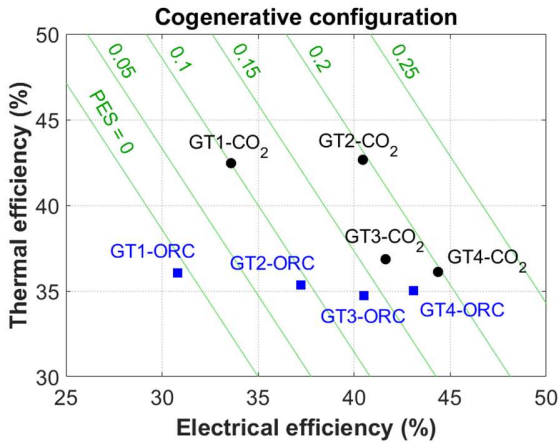


**FIGURE 7: THERMAL EFFICIENCY vs ELECTRIC EFFICIENCY (COG CASE).**

#### 4.1.3 Power production and bottoming cycle design size

For sake of completeness, electric power in both BASE and COG cases and thermal power production data for COG configurations are presented in FIGURE 10. The green line indicates the GT electric power output as standalone unit, for comparison purpose.

Results show that increasing the GT size, increases both the net electric and thermal power production, in COG configurations. Increasing the GT size leads to an increase of the exhaust gas flow rate and thermal power available at the bottomer cycle (see FIGURE 4). Thus, obviously, the bottomer cycle size increases too with the GT size, in all the examined cases. Values of the bottomer cycle power size are presented in TABLE 5.

Results show that combining the bottomer cycle with the GT unit allows to produce additional electric power ranging between about 0.5 MW to 10 MW with the best configuration for electric power production (ORC BASE). Instead, the best configuration for cogenerative purpose, namely s-CO<sub>2</sub> COG, allows to produce at the same time, from 0.6 to 7.3 MW of electric power and from 2.6 to 28.9 MW of thermal power, depending on the GT size.

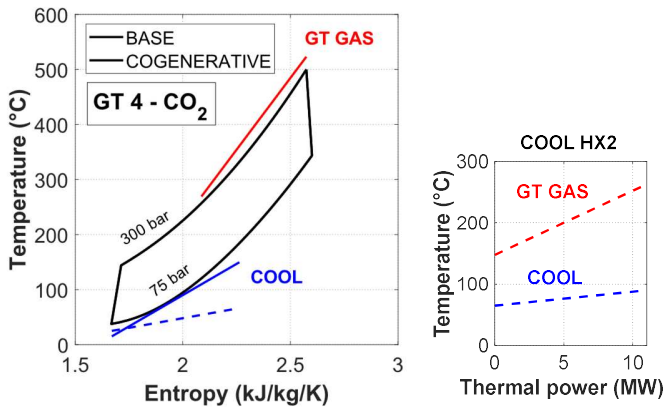


**FIGURE 8: s-CO<sub>2</sub> THERMODYNAMIC T-S DIAGRAM FOR THE BASE AND THE COG CONFIGURATIONS AND COOL HX2 T-Q DIAGRAM (GT4 CASE).**

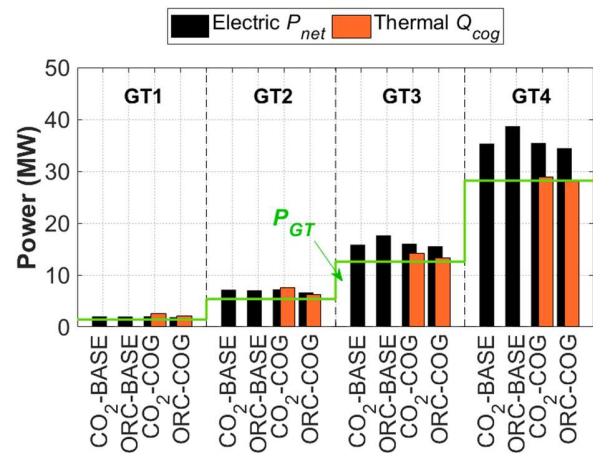


**FIGURE 10: NET ELECTRIC AND THERMAL POWER PRODUCTION FOR THE DIFFERENT CONFIGURATIONS.**

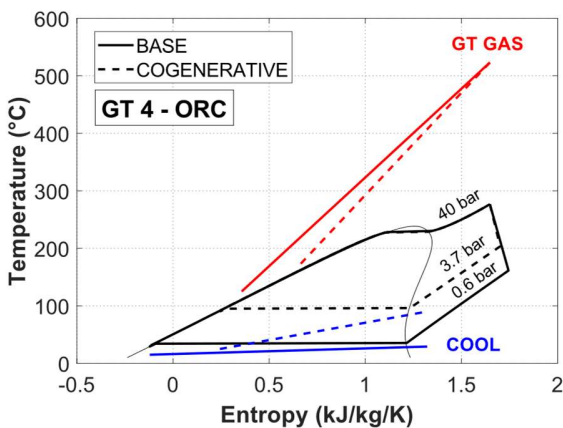


**FIGURE 9: ORC THERMODYNAMIC T-S DIAGRAM FOR THE BASE AND THE COG CONFIGURATIONS (GT4 CASE).**

**TABLE 5: BOTTOMER CYCLE POWER SIZE.**

		Bottomer cycle design size (kW)			
Configuration		GT1	GT2	GT3	GT4
CO <sub>2</sub>	BASE	585	1769	3273	7137
	COG	605	1848	3465	7265
ORC	BASE	576	1653	5066	10502
	COG	434	1256	2970	6256

## 4.2 Size and investment considerations

FIGURE 11 shows values of size parameter of each heat exchanger sections for the different GT-bottomer cycle configurations examined in this study.

The size of the GT unit has a direct influence on the heat exchanger surface area, mainly due to increase in bottoming cycle input thermal power with GT size.

The total surface area is similarly divided among the various heat exchange sections, for given heat recovery configuration, varying the GT in exam. Thus, some considerations can be made on the surface allocation among the different sections. Whilst  $A_{rec}$  is similar for the different configurations, suggesting similar internal heat recovery among the different configurations,  $A_{gas}$  and  $A_{cool}$  can greatly differ. In particular,  $A_{gas}$  value of CO<sub>2</sub> configurations can be more than 4 times the  $A_{gas}$  value of ORC ones, mainly because of the higher convective heat transfer coefficient of cyclopentane into the evaporator, also due to the fluid phase change. Concerning instead COOL HX,  $A_{cool}$  values are more similar between the different configurations. However, a decrease of the size parameter is observed again when using cyclopentane/MM rather than CO<sub>2</sub> as bottoming cycle working fluid.

Values of the total size parameter,  $A_{tot}$ , are compared for the different heat recovery configurations, for given GT model, in order to assess which configuration requires the highest heat exchangers surface areas and consequently the highest investment costs. Therefore, this analysis suggests that higher heat exchangers investment costs can be expected if installing s-CO<sub>2</sub> bottoming cycle rather than ORC, given the higher total size parameter value, which can be more than twice the ORC configuration's one.

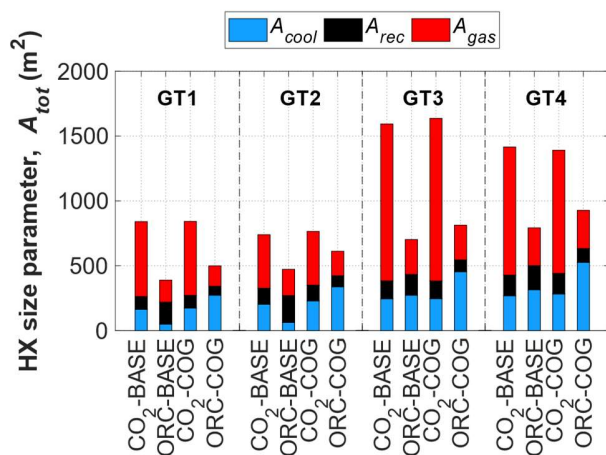


FIGURE 11: HEAT EXCHANGERS SIZE PARAMETERS.

Other considerations derive from the analysis of the second design parameter of interest, i.e. the turbine size parameter.

FIGURE 12 shows the trend of the turbine size parameter as function of the topper GT size, for the different heat recovery configurations. In particular, it can be noticed that comparing the

different bottoming cycle options, the s-CO<sub>2</sub> solution exhibits lower turbine size parameter values, if compared to ORC one, mainly due to the higher density of the fluid passing through the expander. Indeed, the s-CO<sub>2</sub> cycle works at high pressures, comprised between 300 and 75 bar, corresponding to relatively high CO<sub>2</sub> density values that ranges between 500 e 60 kg/m<sup>3</sup> (see FIGURE 13). Cyclopentane and MM, instead, both expand in ORC at lower pressure and lower density (until 1 kg/m<sup>3</sup>), leading to less compact expander machines. It can be noticed that the density of cyclopentane and MM drops markedly in correspondence of the critical temperature value (of about 240°C), because of the fluid phase change.

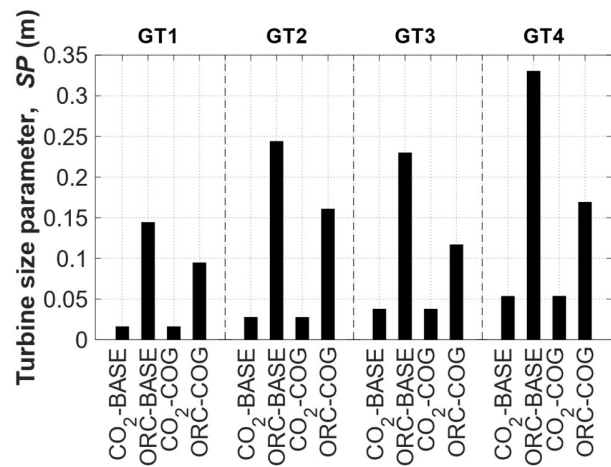


FIGURE 12: TURBINE SIZE PARAMETER.

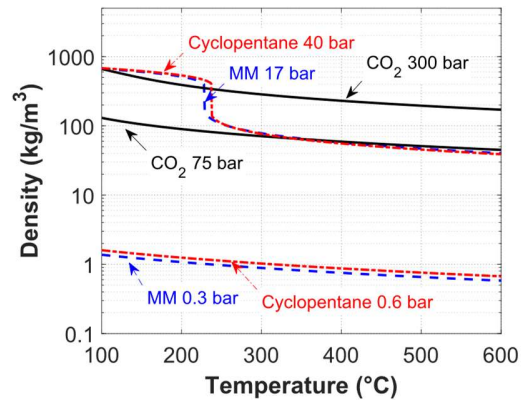


FIGURE 13: WORKING FLUID DENSITY AS FUNCTION OF TEMPERATURE AND PRESSURE.

For given heat recovery solution, turbine size depends also on GT topper size. In particular, it is proportional to GT size, due to the proportionality between the GT size, the bottoming cycle thermal power input and mass flow rate.

Finally, results of a preliminary investment cost assessment are discussed. FIGURE 14 shows how the CO<sub>2</sub> higher GAS HX

surface area leads to higher heat exchangers investment costs for the CO<sub>2</sub> supercritical system if compared to the ORC one. At the same time, the ORC higher turbine size leads to higher expander investment costs for the ORC system if compared to the CO<sub>2</sub> supercritical one.

To determine the most convenient configuration, both these aspects must be taken into account. For this reason, a capital cost parameter is considered, calculated as the sum of the expander and the heat exchangers capital costs. Results show that the highest capital cost parameter is associated to the ORC base configuration and can reach up to 3 million euros when coupled with a 30 MW gas turbine size. According to this study, the CO<sub>2</sub> configuration, instead, could introduce an economical saving of about the 40 %, with respect to the ORC base configuration.

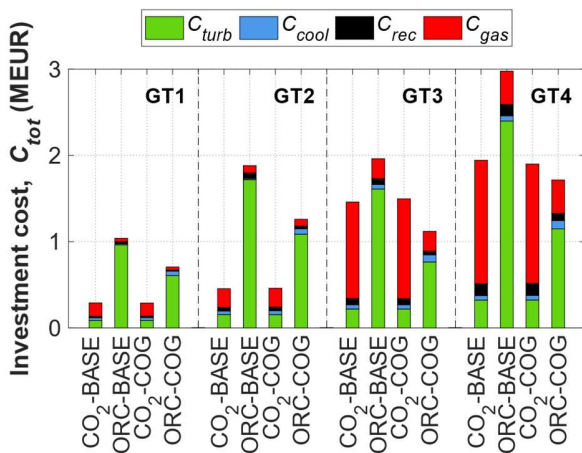


FIGURE 14: CAPITAL COSTS.

## CONCLUSION

This paper presents a systematic comparison between the ORC and the supercritical CO<sub>2</sub> cycle as bottomer of four different size industrial gas turbines (with power sizes from 1 MW to 30 MW), typically employed in the oil and gas sector. Both a base configuration producing electric power only, and a cogenerative configuration providing also thermal power have been analyzed in these scenarios. The different plant solutions have been simulated by means of the commercial software Thermoflex, with the support of the GT PRO gas turbine library. The assumptions related to the bottoming cycles, instead, have been carefully chosen in line with industrial products, experience and technological limits. The results of the simulations comprehend the energy performance analysis, but also some design aspects and investment costs considerations. The results of the comparative analysis can be resumed as following.

Higher recovered thermal powers are observed for the ORC solution, mainly because of the higher convective heat transfer coefficient of cyclopentane and MM into the evaporator and the condenser, also due to the fluid phase change. Despite the ORC exhibit higher recovered thermal power values, the CO<sub>2</sub> solution presents higher isentropic powers available at the expander to

produce work, thanks to the higher pressure difference. However, supercritical CO<sub>2</sub> configurations exhibit also higher operating machine consumption, which corresponds to the 30 % over the expander isentropic power (against the 3 % of the ORC configuration).

Results of the energy analysis considering only the pure electric production, highlight that both the configurations lead to a good increment in the overall net electric efficiency of the power plant, if compared to GT in simple cycle; the average increment is of 9 and 11 percentage points, respectively if considering s-CO<sub>2</sub> or ORC as bottoming solution. However different considerations can be made when considering small-size or larger-size toppler GTs, in particular: s-CO<sub>2</sub> base case is the configuration showing the highest plant net electric efficiency, when combined with small size turbines; instead, when considering larger size GTs, the ORC configuration shows better performance.

Concerning the cogenerative performance, the s-CO<sub>2</sub> system exhibits at the same time higher electric efficiency and thermal efficiency, if compared to ORC system, being equal the installed toppler gas turbine model. The PES values for s-CO<sub>2</sub> cycle range between 10 % and 20 %. The ORC lower performance is due to the high condensing pressure value, imposed by the temperature required by the thermal user.

From the economic point of view, this analysis suggests then that higher heat exchangers investment costs can be expected if installing s-CO<sub>2</sub> bottoming cycle rather than ORC. Opposite considerations derive instead from the turbine size parameter evaluation. Indeed, The ORC working fluid expands into the ORC turbine in lower pressure and lower density ranges, if compared to carbon dioxide into the supercritical cycle, leading to less compact expander machines.

To determine the most convenient configuration, both these aspects must be taken into account. For this reason, a capital cost parameter is considered, calculated as the sum of the expander and the heat exchangers capital costs. [ABBIAMO ESCLUSO COMPRESSORE?] Results show that the highest capital cost parameter is associated to the ORC base configuration and can reach 3 million euros when coupled with a 30 MW gas turbine size. According to this study, the CO<sub>2</sub> configuration, instead, could introduce an economical saving of about the 40 %, with respect to the ORC base configuration.

Results of this work can be good guidelines for a preliminary economic comparison, but they cannot allow to establish a priori the optimal heat recovery configuration from the economic point of view. Further investigation could regard the determination of the economic optimum for more specific applications, accounting for the influence of the yearly demand profile (i.e. gas turbines working profile) on the energetic production, the economic gain, and the final return on the investment.

## REFERENCES

1. Valentini, E.; Bhargava, R.K.; Bianchi, M.; DePascale, A.; Peretto, A. Thermo-Economic Evaluation of ORC System in Off-Shore Applications. Proceedings of ASME Turboexpo 2014, <http://dx.doi.org/10.1115/GT2014-25170>.
2. Campana, F.; Bianchi, M.; Branchini, L.; De Pascale, A.; Peretto, A.; Baresi, M.; Fermi, A.; Rossetti, N.; Vescovo, R. ORC waste heat recovery in European energy intensive industries: Energy and GHG savings. *Energy Convers. Manag.* 2013, 76, 244–252, doi:10.1016/j.enconman.2013.07.041.
3. Redko, A.; Redko, O.; DiPippo, R. 9 - Industrial waste heat resources. In *Low-Temperature Energy Systems with Applications of Renewable Energy*; Redko, A., Redko, O., DiPippo, R., Eds.; Academic Press, 2020; pp. 329–362 ISBN 978-0-12-816249-1.
4. Hedman, B.A. Waste energy recovery opportunities for interstate natural gas pipelines. Report for Interstate Natural Gas Association of America (INGAA) 2008.
5. ORC plants for Oil & Gas stations | TURBODEN Available online: <https://www.turboden.com/solutions/1054/oil-gas>, <https://www.turboden.com/solutions/2603/combined-cycles> (accessed on Oct 14, 2020).
6. Bianchi, M.; Branchini, L.; De Pascale, A.; Melino, F.; Peretto, A.; Torricelli, N.; Kurz, R.; Sanchez, D.; Rossetti, N.; Ferrari, T. Optimal load allocation of compressor drivers taking advantage of Organic Rankine Cycle as WHR solution. Proceedings of ASME Turboexpo 2020.
7. Yu, A.; Su, W.; Lin, X.; Zhou, N. Recent trends of supercritical CO<sub>2</sub> Brayton cycle: Bibliometric analysis and research review. *Nucl. Eng. Technol.* 2020, doi:10.1016/j.net.2020.08.005.
8. Turchi, C.S.; Ma, Z.; Neises, T.W.; Wagner, M.J. Thermodynamic Study of Advanced Supercritical Carbon Dioxide Power Cycles for Concentrating Solar Power Systems. *J. Sol. Energy Eng.* 2013, 135, doi:10.1115/1.4024030.
9. Syblik, J.; Vesely, L.; Entler, S.; Stepanek, J.; Dostal, V. Analysis of supercritical CO<sub>2</sub> Brayton power cycles in nuclear and fusion energy. *Fusion Eng. Des.* 2019, 146, 1520–1523, doi:10.1016/j.fusengdes.2019.02.119.
10. Park, S.; Kim, J.; Yoon, M.; Rhim, D.; Yeom, C. Thermodynamic and economic investigation of coal-fired power plant combined with various supercritical CO<sub>2</sub> Brayton power cycle. *Appl. Therm. Eng.* 2018, 130, 611–623, doi:10.1016/j.applthermaleng.2017.10.145.
11. Liu, Y.; Wang, Y.; Huang, D. Supercritical CO<sub>2</sub> Brayton cycle: A state-of-the-art review. *Energy* 2019, 189, 115900, doi:10.1016/j.energy.2019.115900.
12. Astolfi, M.; Alfani, D.; Lasala, S.; Macchi, E. Comparison between ORC and CO<sub>2</sub> power systems for the exploitation of low-medium temperature heat sources. *Energy* 2018, 161, 1250–1261, doi:10.1016/j.energy.2018.07.099.
13. *Thermoflex 28.0. Sudbury, MA, USA: Thermoflow Inc; 2017;*
14. Crespi, F.; Sanchez, D.; Gavagnin, G.; Martinez, G.S. Analysis of the Thermodynamic Potential of Supercritical Carbon Dioxide Cycles: A Systematic Approach. 2017, 14.
15. Bhargava, R.K.; Bianchi, M.; Branchini, L.; Pascale, A.D.; Orlandini, V. Organic Rankine Cycle System for Effective Energy Recovery in Offshore Applications: A Parametric Investigation With Different Power Rating Gas Turbines. Proceedings of ASME Turboexpo 2015. <https://doi.org/10.1115/GT2015-42292>
16. Bianchi, M.; Branchini, L.; De Pascale, A.; Melino, F.; Peretto, A.; Archetti, D.; Campana, F.; Ferrari, T.; Rossetti, N. Feasibility of ORC application in natural gas compressor stations. *Energy* 2019, 173, 1–15, doi:10.1016/j.energy.2019.01.127.
17. Eric W. Lemmon, Ian H. Bell, Marcia L. Huber, and Mark O. McLinden *REFPROP 10.0 Standard Reference Database 23*; National Institute of Standards and Technology, Boulder, Colorado, United States;
18. Directive 2004/08/EC of the European Parliament and of the Council, Official Journal of the European Union 21.2.2004, pp. 50–60.
19. Green, D.D.W.; Southard, D.M.Z. *Perry's Chemical Engineers' Handbook, 9th Edition*; McGraw-Hill Education, 2019; ISBN 978-0-07-183408-7.
20. *Organic Rankine cycle (ORC) power systems: technologies and applications*; Macchi, E., Astolfi, M., Eds.; Woodhead Publishing series in energy; Woodhead Publishing is an Imprint of Elsevier: Duxford; Cambridge, Massachusetts; Kidlington, 2017; ISBN 978-0-08-100510-1.
21. Astolfi, M.; Romano, M.C.; Bombarda, P.; Macchi, E. Binary ORC (Organic Rankine Cycles) power plants for the exploitation of medium–low temperature geothermal sources – Part B: Techno-economic optimization. *Energy* 2014, 66, 435–446, doi:10.1016/j.energy.2013.11.057.